Biochimica et Biophysica Acta 1832 (2013) 1463–1472

Contents lists available at SciVerse ScienceDirect

Biochimica et Biophysica Acta

journal homepage: www.elsevier.com/locate/bbadis

Acute renal proximal tubule alterations during induced metabolic crises in a mouse model of glutaric aciduria type 1

Bastian Thies [a,1], Catherine Meyer-Schwesinger [b,1], Jessica Lamp [a], Michaela Schweizer [c], David M. Koeller [d], Kurt Ullrich [a], Thomas Braulke [a], Chris Mühlhausen [a,*]

[a] Children's Hospital, Department of Biochemistry, University Medical Center Hamburg-Eppendorf, Hamburg, Germany
[b] Department of Internal Medicine III, Nephrology and Rheumatology, University Medical Center Hamburg-Eppendorf, Hamburg, Germany
[c] Center for Molecular Neurobiology (ZMNH), University Medical Center Hamburg-Eppendorf, Hamburg, Germany
[d] Department of Pediatrics, Oregon Health and Science University, Portland, OR 97239, USA

ARTICLE INFO

Article history:
Received 4 March 2013
Received in revised form 16 April 2013
Accepted 17 April 2013
Available online 24 April 2013

Keywords:
Glutaric aciduria type 1
Metabolic disease
Acute tubular injury
Dicarboxylate transporter
Transporter expression

ABSTRACT

The metabolic disorder glutaric aciduria type 1 (GA1) is caused by deficiency of the mitochondrial glutaryl-CoA dehydrogenase (GCDH), leading to accumulation of the pathologic metabolites glutaric acid (GA) and 3-hydroxyglutaric acid (3OHGA) in blood, urine and tissues. Affected patients are prone to metabolic crises developing during catabolic conditions, with an irreversible destruction of striatal neurons and a subsequent dystonic–dyskinetic movement disorder. The pathogenetic mechanisms mediated by GA and 3OHGA have not been fully characterized. Recently, we have shown that GA and 3OHGA are translocated through membranes *via* sodium-dependent dicarboxylate cotransporter (NaC) 3, and organic anion transporters (OATs) 1 and 4. Here, we show that induced metabolic crises in *Gcdh*$^{-/-}$ mice lead to an altered renal expression pattern of NaC3 and OATs, and the subsequent intracellular GA and 3OHGA accumulation. Furthermore, OAT1 transporters are mislocalized to the apical membrane during metabolic crises accompanied by a pronounced thinning of proximal tubule brush border membranes. Moreover, mitochondrial swelling and increased excretion of low molecular weight proteins indicate functional tubulopathy. As the data clearly demonstrate renal proximal tubule alterations in this GA1 mouse model during induced metabolic crises, we propose careful evaluation of renal function in GA1 patients, particularly during acute crises. Further studies are needed to investigate if these findings can be confirmed in humans, especially in the long-term outcome of affected patients.

1. Introduction

Glutaric aciduria type 1 (GA1) is an autosomal-recessively inherited inborn error in the degradative pathway of the amino acids lysine, hydroxylysine and tryptophan, caused by deficiency of the mitochondrial matrix enzyme glutaryl-CoA dehydrogenase (GCDH). GCDH deficiency leads to the accumulation of the pathologic metabolites glutaric (GA) and 3-hydroxyglutaric (3OHGA) acids in tissues and body fluids. Affected patients are prone to the development of metabolic crises precipitated by catabolic states during a time window of vulnerability between 6 and 36 months of age, with an irreversible destruction of striatal neurons and a subsequent dystonic–dyskinetic movement disorder. The symptomatic treatment consists of an adequate emergency management during catabolic situations, a lysine-restricted diet and supplementation of carnitine to promote the coupling and urinary excretion of GA and 3OHGA [1,2].

The pathomechanisms leading to neurodegeneration in GA1 are unknown. GA- and 3OHGA-mediated activation of N-methyl-D-aspartate (NMDA) receptors, the inhibition of synthesis of the neurotransmitter γ-aminobutyric acid (GABA), the impairment of mitochondrial energy production, and the disintegration of endothelial barriers have been reported in various *in vitro* and *in vivo* models [3–7].

A GCDH-deficient mouse model displays the biochemical hallmarks of the GA1 disease [8], and the administration of a high protein diet (HPD) to 4-week-old [9] or 6-week-old [10] *Gcdh*$^{-/-}$ mice leads to the development of metabolic crises with a further increase of GA and 3OHGA concentrations in tissues and urine.

Several members of the dicarboxylate transporter family have been identified to mediate the translocation of GA and 3OHGA

Abbreviations: GA, glutaric acid; GA1, glutaric aciduria type 1; GABA, γ-aminobutyric acid; GCDH, glutaryl-CoA dehydrogenase; HPD, high protein diet; HNF, hepatocyte nuclear factor; MUP1, major urinary protein 1; NaC, sodium-dependent dicarboxylate cotransporter; ND, normal diet; NHERF, sodium hydrogen exchanger regulatory factor; NMDA, N-methyl-D-aspartate; OAT, organic anion transporter; OATP, organic anion transporting polypeptide; 3OHGA, 3-hydroxyglutaric acid; PAS, periodic acid-Schiff; RST, renal-specific transporter; SLC, solute carrier; WGA, wheat germ agglutinin; WT, wild-type

* Corresponding author at: Children's Hospital, Department of Biochemistry, University Medical Center Hamburg-Eppendorf, Martinistrasse 52, Building N27, 20246 Hamburg, Germany. Tel.: +49 40 7410 57188; fax: +49 40 7410 55053.
E-mail address: muehlhausen@uke.de (C. Mühlhausen).

[1] These authors contributed equally to the work.

0925-4439/$ – see front matter © 2013 Elsevier B.V. All rights reserved.
http://dx.doi.org/10.1016/j.bbadis.2013.04.019

through membranes [11,12]. In particular, the urinary excretion of the metabolites GA and 3OHGA is facilitated by the concerted action of the sodium-dependent dicarboxylate co-transporter 3 (NaC3, Slc13a3) and the organic anion transporter (OAT) 1 (Slc22a6) at the basolateral site, and OAT4 (Slc22a11) at the apical membrane, of GCDH-expressing renal proximal tubule cells [13]. Almost no data, however, are available on the expression and regulation of these transporters in kidney cells of *Gcdh*$^{-/-}$ mice during HPD-induced metabolic crises, and the consequences of acute HPD-induced crises on the morphology and function of the kidney. A single GA1 patient with an early onset of neurologic disease, accompanied by a congenital nephrotic syndrome with acute glomerulonephritis, rapidly progressive renal failure and death has been described [14]. Interestingly, *Gcdh*$^{-/-}$ mice under basal conditions display a significant enlargement of kidneys [8] and during HPD-induced metabolic crises an accumulation of 3OHGA in kidney cells [10,11].

In the present study, we investigated the mRNA expression of *NaC3*, *Oat1*, *Oat2* (Slc22a7, the murine equivalent of human OAT4), the organic anion transporting polypeptide (*Oatp*) 1a6 (Slc21a13), and the renal-specific transporter (*Rst*, Slc22a12), the murine ortholog of the human urate transporter URAT1, as well as the protein expression and immunohistochemical distribution of OAT1. Furthermore, we performed ultrastructural analyses of mouse kidneys as well as functional investigations of mouse urine, both under basal conditions and during induced metabolic crises.

Here we show that during induced metabolic crises, the mRNA expression of *Oat1* and *Oat2* is increased and decreased, respectively, which likely contributes to the intracellular accumulation of pathologic metabolites in the kidney of *Gcdh*$^{-/-}$ mice previously reported [10]. Furthermore, we demonstrate that the metabolic crises result in an increase of OAT1 protein and its mislocalization from the basolateral to the apical membrane, accompanied by loss of proximal tubule brush border membranes, and ultrastructural changes of mitochondria in renal proximal tubule cells. Beyond that, during induced metabolic crises the pattern of proteins excreted into urine by *Gcdh*$^{-/-}$ mice indicates the presence of tubulopathy.

2. Materials and methods

2.1. Mice

Gcdh$^{-/-}$ mice and wild-type littermate controls were generated from heterozygotes [8]. The genetic background of all mice groups used in this study was C57BL6/SJ129 hybrid. The genotypes were confirmed by polymerase chain reaction (PCR) and measurements of glutarylcarnitine concentration in dried blood spots. The mice were housed in an animal facility of the University Hospital with a 12-h light–dark cycle and allowed water and food *ad libitum*. Animal care was provided in accordance with institutional guidelines. Anesthetized mice were used for preparation of kidneys, perfused for electron microscopy or immunohistochemistry as described below. Special mice food with high protein content (70% casein) was purchased from Harlan Laboratories (Indianapolis, IN, USA). Mice were fed with this special diet until they displayed symptoms of an induced metabolic crisis [9]. Urine was collected in metabolic cages 3600M009 from Tecniplast (Hohenpeißenberg, Germany).

2.2. Antibodies and reagents

Polyclonal anti-organic anion transporter 1 antibody raised in rabbits was from Alpha Diagnostic International (San Antonio, TX, USA), polyclonal anti-retinol binding protein (RBP) was kindly provided by C. Hübner (University of Jena, Germany), polyclonal anti-major urinary protein 1 (MUP1) from Santa Cruz (Heidelberg, Germany), guinea pig-anti-nephrin from Acris (Herford, Germany), rabbit-anti-MnSOD from Millipore (Temecula, CA, USA). Horseradish peroxidase (HRP)-conjugated anti-rabbit-IgG, CY2-conjugated rabbit-anti-guinea pig-IgG and CY2-conjugated donkey-anti-rabbit-IgG were from Jackson ImmunoResearch Laboratories (West Grove, PA, USA). ToPro3® was from Invitrogen/Molecular Probes (Carlsbad, CA, USA) and Texas red wheat germ agglutinin from Vector (Burlingame, CA, USA).

2.3. RNA extraction, cDNA preparation and real-time PCR

Total ribonucleic acid (RNA) was prepared from mice kidneys with TRI® Reagent from Applied Biosystems/Ambion (Austin, TX, USA) followed by phenol–chloroform extraction according to the manufacturer's instructions. RNA was reverse transcribed into cDNA using High-Capacity cDNA Reverse Transcription Kit (Life Technologies/Applied Biosystems, Carlsbad, CA, USA). Quantitative RT-PCR was performed using Mx3000P™ QPCR System from Agilent Technologies/Stratagene (Santa Clara, CA, USA). Maxima® Probe qPCR Master Mix from Thermo Scientific/Fermentas (Waltham, MA, USA) and TaqMan® Gene Expression Assays (Life Technologies/Applied Biosystems, Carlsbad, CA, USA) were used. TaqMan assay ID numbers are listed in the supplementary methods (Supplementary Table 1). The relative level of each mRNA was determined using the comparative CT method [15].

2.4. Western blotting

Membrane protein fractions were extracted by homogenization of 100 mg of mouse kidney tissue in 500 μl 50 mM Tris–HCl pH 7.4 containing 2 mM EDTA and 2% proteinase inhibitor cocktail (Sigma, Deisenhofen, Germany) with a 20-gauge needle followed by centrifugation at 1000 ×*g* for 5 min at 4 °C. The postnuclear supernatant was centrifuged at 100,000 ×*g* for 30 min at 4 °C, and the pelleted membranes resuspended by addition of 200 μl of 10 mM phosphate-buffered saline pH 7.4 containing 0.5% Triton X-100 (Sigma) and 2% proteinase inhibitor cocktail and subsequent ultrasonification. The homogenate was centrifuged at 100,000 ×*g* for 30 min at 4 °C, the supernatant collected and protein concentration calculated with the BioRad protein assay (Munich, Germany). Membrane protein extracts (250 μg of protein) were used for Western blotting with anti-OAT1 (0.17 μg/ml) or anti-MnSOD antibody (1:1 000) and visualized with HRP-conjugated anti-rabbit IgG (1:5 000) and enhanced chemiluminescence reagents. Urine aliquots corresponding to an amount of 1 μg creatinine were used for SDS-PAGE and Western blotting with anti-Retinol Binding Protein antibody (1:250) or anti-MUP1 antibody (1:200), and visualized with HRP-conjugated anti-rabbit IgG (1:5 000) and enhanced chemiluminescence reagents.

2.5. Histology and immunohistochemistry in kidneys of *Gcdh*$^{-/-}$ and wild-type mice

Whole kidneys were perfused, fixed in 4% buffered formalin for 24 h, and embedded in paraffin (Medim Histotechnologie, Buseck, Germany). Deparaffinized and rehydrated sections (2 μm) were either stained by the periodic acid-Schiff (PAS) reaction or processed for immunohistochemical stainings. Antigen retrieval was performed by microwave antigen retrieval in citrate buffer, pH 6.1 for 25 min (nephrin) or in DAKO antigen retrieval buffer pH 9.0 for 15 min at 98 °C in a steam cooker. After blocking in 5% horse serum (Vector) for 30 min, the tissue was incubated with primary antibodies (anti-nephrin 1:100; anti-OAT1, 1:200) in 5% horse serum over night at 4 °C. For double immunofluorescence microscopy, antibody binding was visualized using affinity purified CY2-conjugated secondary antibodies diluted 1:400 in 5% horse serum for 30 min. ToPro3 (1:2000) was used for nuclear staining and Texas red-coupled wheat germ agglutinin (1:400) for counterstaining of apical membranes. Stainings were evaluated under an Axioskop (Zeiss, Jena, Germany) and photographed with an Axiocam HRc (Zeiss) or by confocal microscopy with a LSM 510 meta microscope using the LSM software.

Micrographs were analyzed with Adobe Photoshop 7.0 software (Adobe, San Jose, CA, USA).

2.6. Electron microscopy

Mice were deeply anesthetized with an intraperitoneal injection of sodium pentobarbital 100 mg/kg. A fixative solution of 4% paraformaldehyde and 1% glutaraldehyde in 0.1 M phosphate buffer at pH 7.2–7.4 was perfused transcardially. The kidneys of the perfused mice were immediately submerged in a solution of the same fixative and stored overnight. 150 μm thick Vibratom sections were cut with a vibratome (Leica VT 1000S). The sections were rinsed three times in 0.1 M sodium cacodylate buffer (pH 7.2–7.4) and osmicated using 1% osmium tetroxide in cacodylate buffer. Following osmication, the sections were dehydrated using ascending ethyl alcohol concentration steps, followed by two rinses in propylene oxide. Infiltration of the embedding medium was performed by immersing the pieces in a 1:1 mixture of propylene oxide and Epon and finally in neat Epon and hardened at 60 °C. Semithin sections (0.5 μm) were prepared for LM mounted on glass slides and stained for 1 min with 1% toluidine blue. Ultrathin sections (60 nm) were cut and mounted on copper grids. Sections were stained using uranyl acetate and lead citrate. Thin sections were examined and photographed using an EM902 (Zeiss) electron microscope.

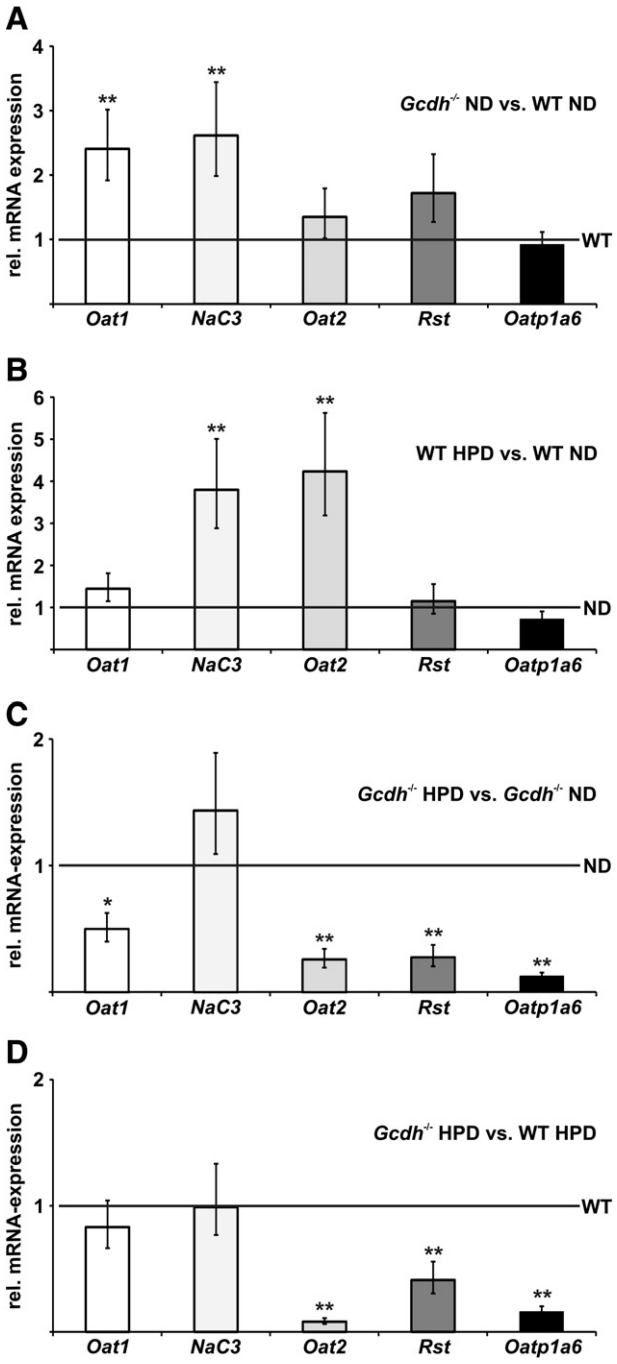

Fig. 1. mRNA expression of renal transporters. The relative mRNA expression of *NaC3* and the organic anion transporters *Oat1*, *Oat2*, *Rst*, and *Oatp1a6* was tested in kidney tissues of wild-type (WT) or *Gcdh*$^{-/-}$ mice under ND or HPD administered for four days, and compared to each other as indicated. The mRNA expression of the respective reference condition (WT or ND) was assigned as 1, indicated by horizontal black lines. Bars indicate relative mRNA expressions (mean ± SD; RNA of kidney tissues of three mice per group were prepared and measured in triplicates). Significance was tested by one-way analysis of variance followed by least significant difference test; *$p < 0.05$, **$p < 0.01$.

2.7. TUNEL staining

In order to detect apoptotic tubular cells in *Gcdh*$^{-/-}$ mice after the high protein diet challenge, TUNEL stainings were performed using the ApopTag Fluorescein *in situ* apoptosis detection kit (Millipore/Chemicon, Billerica, MA, USA) according to the manufacturer's instructions. Briefly, 3 μm paraffin sections were deparaffinized and rehydrated. Antigen retrieval was performed using proteinase K (20 μg/ml, Sigma) for 15 min at RT. Working strength TdT (terminal deoxynucleotidyl transferase) enzyme was added for 2 h at 37 °C to modify apoptotic DNA fragments with digoxigenin-labeled nucleotides. Digoxigenin-labels were visualized using working strength fluorescein-conjugated anti digoxigenin antibody. ToPro3 (1:2 000) was used for nuclear staining. Stainings were evaluated with a LSM 510 meta microscope (Zeiss, Jena, Germany) using the LSM software. Sections of wild-type mouse kidneys treated with DNAse (1 μg/ml, 30 min at 37 °C) were used as apoptose-positive controls.

2.8. Albumin and creatinine quantification in urine

Urine albumin content was quantified using a commercially available ELISA system (Bethyl, Montgomery, TX, USA) according to the manufacturer's instructions using an ELISA plate reader (BioTek, EL 808) as described [16]. The urinary albumin concentration was calculated according to the formula for absorption = $(A - D) / 1 + (x / C)^B + D)$, where A and D are values from the standard curve. Regression values for the standard curve with *r-values* > 0.9950 indicated accurate measurements. Urinary albumin values were standardized against urine creatinine values of the same animals. Urine pH, glucose and creatinine concentrations were determined by routine

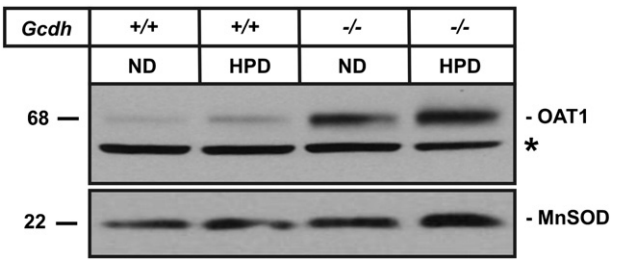

Fig. 2. OAT1 protein expression in mouse kidney. Extracts of kidney tissues (250 μg protein) derived from 42 day-old wild-type (+/+) or *Gcdh*-deficient (−/−) mice treated with ND or HPD for four days were analyzed by OAT1 Western blotting (n = 2). The mitochondrial protein manganese-dependent superoxide dismutase (MnSOD) was used as loading control. *Unspecific Oat1-immunoreactive band.

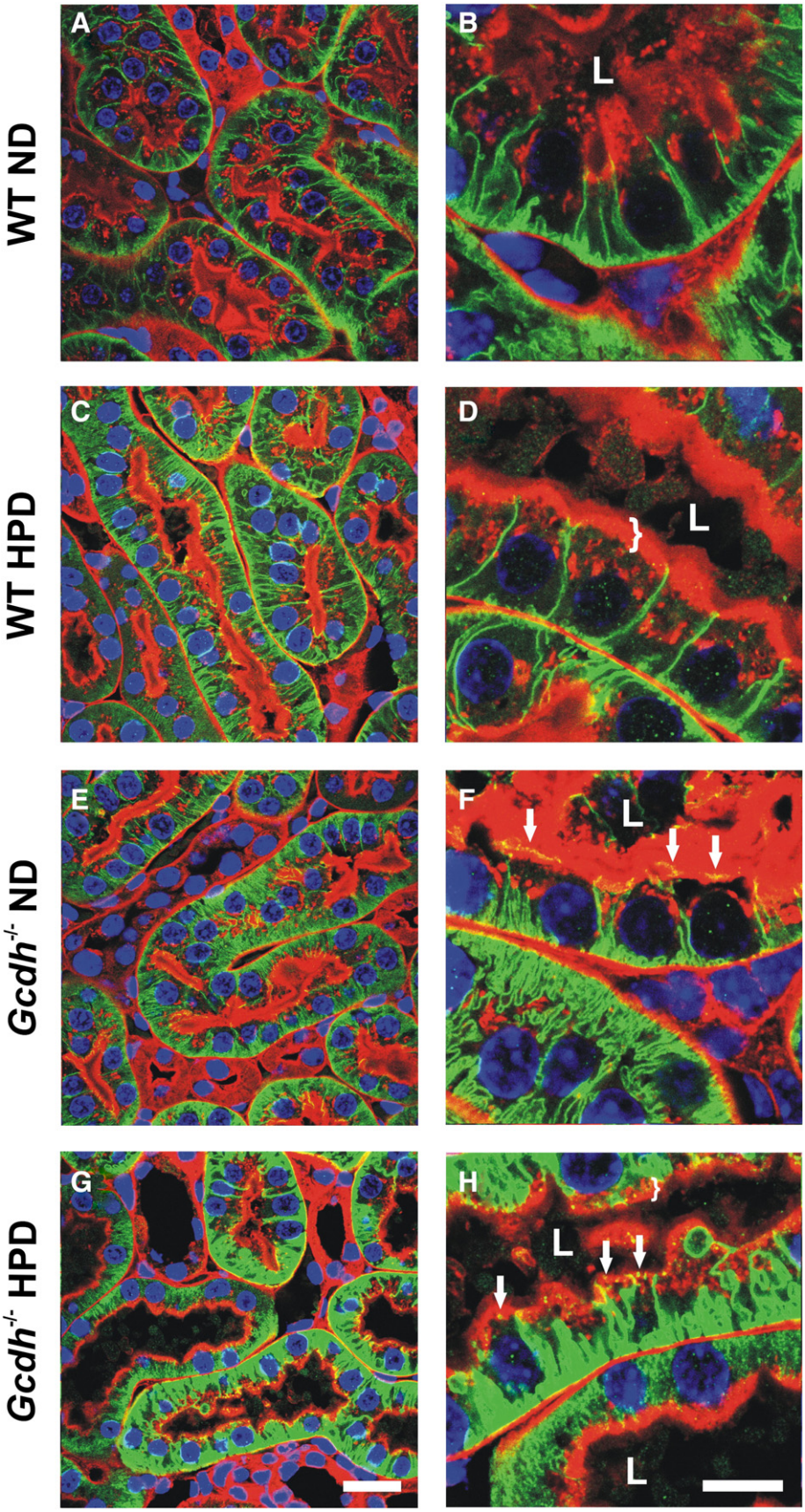

Fig. 3. High expression of OAT1 at basolateral membranes of proximal tubule cells in *Gcdh*$^{-/-}$ mice. Kidneys were prepared from 42 day-old wild-type and *Gcdh*$^{-/-}$ littermates after 4 days of ND and HPD. Kidney sections (2 μm) of wild-type (A–D) and *Gcdh*$^{-/-}$ (E–H) mice were analyzed for OAT1 immunoreactivity (green). Apical membranes of proximal tubule cells were labeled by wheat germ agglutinin-Texas red (red). Nuclei are stained by ToPro3 (blue). Bar length: 20 μm (A, C, E, G), and 10 μm (B, D, F, H). L: proximal tubule lumen. Arrows indicate colocalizations of OAT1 with wheat germ agglutinin-Texas red. Brackets (D, H) mark the thickness of tubule brush border membrane.

methods in the Department of Clinical Chemistry of the University Medical Center Hamburg-Eppendorf.

2.9. Silver staining of urine

Urine aliquots corresponding to an amount of 1 μg creatinine were loaded on SDS-PAGE. Protein staining was performed by silver staining as described previously [17].

2.10. Data analysis

Data were analyzed using one-way analysis of variance followed by Least Significant Difference Test. Significance was accepted at $p < 0.05$. SPSS 12.0 software (SPSS, Chicago, IL, USA) was used for calculations.

3. Results

3.1. Altered mRNA expression of renal transporters in Gcdh$^{-/-}$ mice during induced metabolic crises

Recently, we have reported on an upregulation of *NaC3* mRNA expression in kidneys of *Gcdh*$^{-/-}$ mice under basal conditions in comparison with wild-type mice [11]. To examine the effect of induced metabolic crises, the renal transcript levels of *NaC3*, *Oat1* and *Oat2* (the murine equivalent of hOAT4) were measured after a four day administration of a normal diet (ND) and a high protein diet (HPD) in 42 day-old wild-type and *Gcdh*$^{-/-}$ mice. As controls mRNA expression of *Rst* and *Oatp1a6*, which are organic anion transporters not involved in GA and 3OHGA translocation, were determined.

In addition to *NaC3*, the mRNA expression of *Oat1* was 2.4-fold upregulated in the kidney of *Gcdh*$^{-/-}$ mice under ND as compared to wild-type mice (Fig. 1A; [11]. The renal expression of *Oat2*, *Rst* and *Oatp1a6* did not differ between wild-type and *Gcdh*$^{-/-}$ mice on ND. The administration of HPD to wild-type animals increased the mRNA expression of *NaC3* as well as *Oat2* 3.8- and 4.2-fold, respectively (Fig. 1B), whereas the expression of the other transporters tested remained unchanged. In *Gcdh*$^{-/-}$ mice the HPD resulted in a small but not significant increase in *NaC3* expression (range 1.1- to 1.9-fold, Fig. 1C), whereas the expression of *Oat1*, *Oat2*, *Rst* and *Oatp1a6* decreased (50, 26, 28, and 13%, respectively) relative to *Gcdh*$^{-/-}$ mice on the ND (Fig. 1C). To evaluate whether these effects resemble specific alterations of *Gcdh*$^{-/-}$ mice during induced metabolic crises, or rather represent unspecific findings due to administration of HPD alone, the mRNA expressions of transporters in *Gcdh*$^{-/-}$ mice on HPD were compared directly to wild-type animals on HPD (Fig. 1D). These data revealed comparable results (Fig. 1D *versus* C), indicating that the observed alterations in transporter mRNA expression are effects specifically attributable to the induced metabolic crisis in *Gcdh*$^{-/-}$ mice.

3.2. OAT1 protein expression in kidney tissue of Gcdh$^{-/-}$ mice during induced metabolic crises

To examine whether the altered levels of *Oat1*-mRNA correlate with altered OAT1 protein expression, Western blot analyses were performed. As shown in Fig. 2, in animals on the ND the level of OAT1 protein was significantly increased in kidneys of *Gcdh*$^{-/-}$ mice in comparison to wild-type animals. The administration of an HPD resulted in a slight increase of renal OAT1 protein level in wild-type mice, whereas the OAT1 protein content in kidneys of *Gcdh*$^{-/-}$ mice was further augmented in comparison to a normal diet (Fig. 2).

When the localization of OAT1 was examined by double immunofluorescence histochemistry, OAT1 was found at the basolateral membrane of proximal tubules of wild-type mice as expected on both ND (Fig. 3A, B), and the HPD (Fig. 3C, D). In contrast, OAT1-immunoreactive staining intensity was strongly increased in *Gcdh*$^{-/-}$ mice under ND (Fig. 3E, F), and further increased by HPD administration in comparison to wild-type littermates (Fig. 3G, H). Additionally, HPD treatment led to a mislocalization of OAT1 to apical membranes of proximal tubule cells stained by wheat germ agglutinin (WGA)-Texas red in *Gcdh*$^{-/-}$ mice (Fig. 3F, H, arrows). In addition, the WGA-Texas red staining clearly demonstrates a marked thinning of the proximal tubular brush border under conditions of HPD in *Gcdh*$^{-/-}$ mice (Fig. 3D *vs*. H, brackets; Supplementary Fig. 1).

3.3. Time course of renal transporter mRNA expression during induced metabolic crises

To examine whether the observed mRNA downregulation of *Oat2* and *Rst* expressed at the apical membrane of proximal tubule cells [18,19], and of *Oatp1a6* after four days of HPD treatment is an immediate or later response, their mRNA expressions in *Gcdh*$^{-/-}$ mice

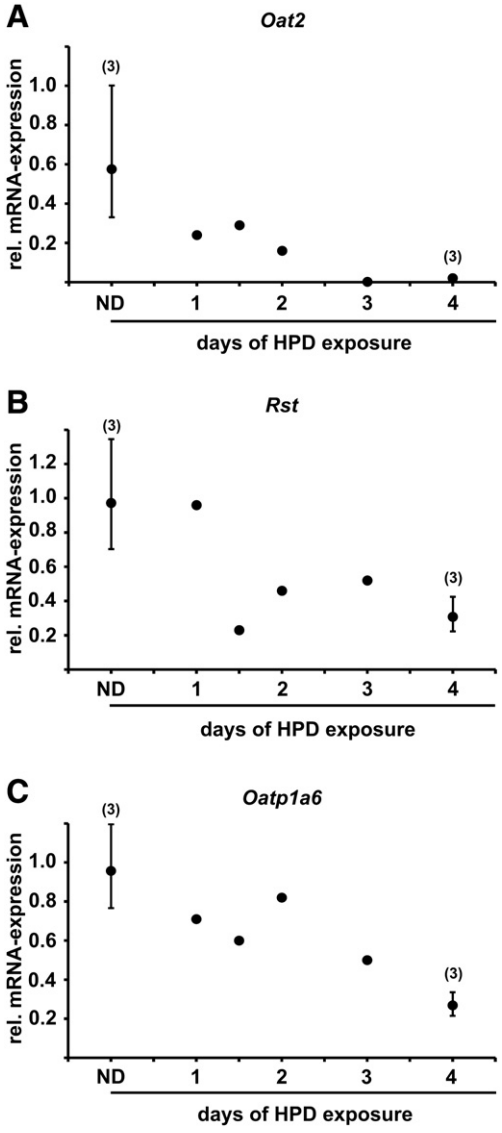

Fig. 4. Time course of mRNA expression of renal transporters during induced metabolic crises. The *Oat2* (A), *Rst* (B), and *Oatp1a6* (C) mRNA expression was analyzed every day after start of HPD administration to *Gcdh*$^{-/-}$ mice as compared to wild-type mice on ND. Dots display mean values of three experiments (each carried out in triplicates, performed with RNA derived from three different mice per group), or values of single experiments (carried out in triplicate 1, 1.5, 2 and 3 days after start of HPD), as compared to the respective mRNA level of wild-type mice on ND.

were tested every day of the diet and related to the respective mRNA expression in wild-type mice on ND. The relative mRNA expressions of *Oat2* and *Oatp1a6* decreased in a linear manner (Fig. 4A and C), whereas the decrease in *Rst* transcript level was slightly delayed (Fig. 4B).

3.4. Histologic alterations in kidneys during induced metabolic crises

PAS staining was performed in order to evaluate light microscopic alterations in kidneys of *Gcdh*$^{-/-}$ mice in comparison to wild-type mice under conditions of ND or HPD. Glomeruli appeared normal on both diets in *Gcdh*$^{-/-}$ and wild-type mice (Fig. 5A–D). In nephrons, a significant loss of the apical brush border was visible along the convoluted and straight parts of the proximal tubules of *Gcdh*$^{-/-}$ mice on HPD (Fig. 5D, Supplementary Fig. 2). Proximal tubular cells appeared vacuolated in some regions (Supplementary Fig. 2), and a negligible fraction of the tubules were occluded by protein casts. No changes along the distal tubules or collecting duct tubules could be observed by light microscopic evaluation (data not shown).

To further evaluate alterations of proximal tubule cells (Fig. 5D), ultrathin sections of kidneys were prepared and analyzed by electron microscopy. The ultrastructure of renal proximal tubules from wild-type mice on ND and HPD, and *Gcdh*$^{-/-}$ on ND showed no abnormalities (Fig. 6A–F). In contrast, ultrathin sections derived from *Gcdh*$^{-/-}$ mice after 4 days of HPD treatment showed enlarged and electron lucent mitochondria in renal proximal tubule cells (Fig. 6G, H). Quantitative analysis of the size of mitochondria confirmed a significant 4-fold enlargement of mitochondria in HPD-treated *Gcdh*$^{-/-}$ mice when compared to *Gcdh*$^{-/-}$ mice on ND or wild-type animals on either diet ($1.57 \pm 1.2\ \mu m^2$ *vs.* $0.38 \pm 0.3\ \mu m^2$; respectively; $p < 0.001$; $n = 321$ wild-type mitochondria, $n = 224$ *Gcdh*$^{-/-}$ mitochondria; Supplementary Fig. 3).

To evaluate the glomerular filtration barrier nephrin immunohistochemistry was performed, which demonstrated no abnormalities in *Gcdh*$^{-/-}$ mice on either diet, indicating that podocyte foot processes and podocyte morphology were not altered in any of the conditions tested (Supplementary Fig. 4). In addition, no significant tubular apoptosis was detected in *Gcdh*$^{-/-}$ mice on ND or after administration of HPD in comparison to wild-type control mice, examined by TUNEL assay (Supplementary Fig. 5).

3.5. Urinary protein excretion in wild-type and *Gcdh*$^{-/-}$ mice

To test whether the alterations in transporter expression and localization in kidneys of *Gcdh*$^{-/-}$ mice on HPD are accompanied by functional abnormalities, the protein composition of urine from wild-type and *Gcdh*$^{-/-}$ mice during the four-day administration of ND and HPD was analyzed. Wild-type mice displayed a uniform excretion of an 18 kDa protein on ND as well as during administration of HPD for 4 days (Fig. 7). In urines of *Gcdh*$^{-/-}$ mice on ND or HPD the excretion of the 18 kDa polypeptide was strongly decreased. In addition, *Gcdh*$^{-/-}$ mice on HPD showed a low molecular weight proteinuria from the first day of HPD treatment. Western blot analyses showed that the 18 kDa polypeptide corresponded to mouse major urinary protein 1 (MUP1) and confirmed the decrease in MUP1 excretion in *Gcdh*$^{-/-}$ mice as compared to wild-type animals (Supplementary Fig. 6).

Further analyses of urine revealed no differences in the excretion of retinol binding protein (RBP, data not shown), or albumin (Supplementary Fig. 7). There were also no differences in urine pH (pH 5.6 ± 0.5 and 5.4 ± 0.5, respectively) or glucose content (data not shown) between wild-type and *Gcdh*$^{-/-}$ mice on the HPD.

4. Discussion

Here we have shown that a metabolic crisis induced by a high protein diet in *Gcdh*$^{-/-}$ mice leads to i) altered expression of NaC3 and OAT1 transporters mediating the translocation of the pathologic metabolites GA and 3OHGA, ii) mislocalization of OAT1 to apical membranes of

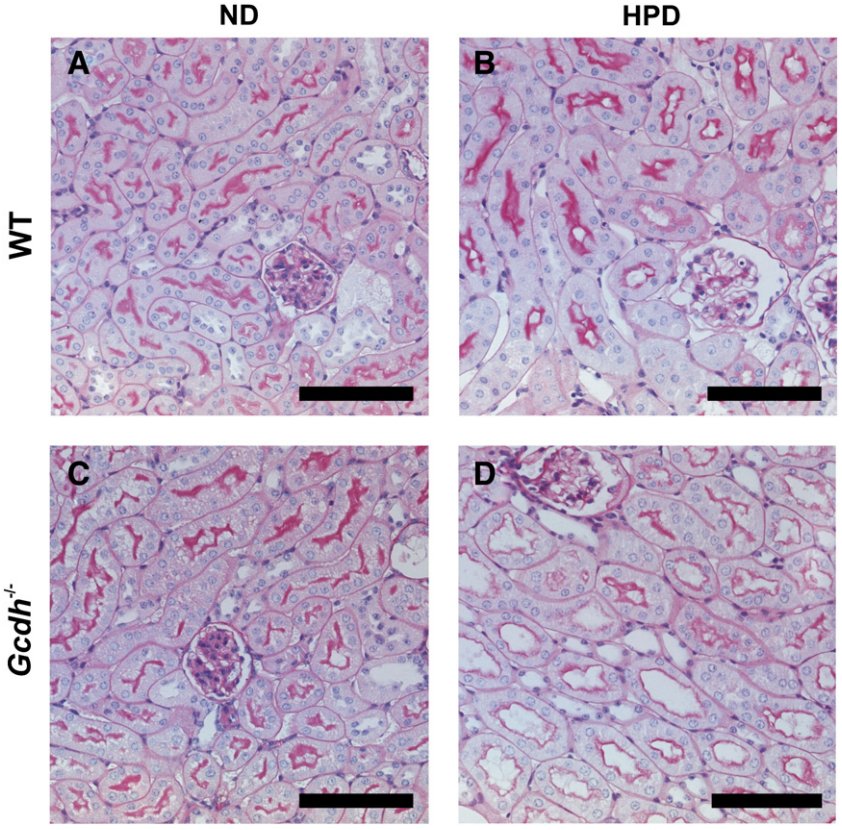

Fig. 5. PAS staining of kidneys of *Gcdh*$^{-/-}$ and wild-type mice. PAS stainings of 2 μm kidney sections of 42 day-old wild-type (A, B) and *Gcdh*$^{-/-}$ mice (C, D) after four-day administration of ND (A, C) and HPD (B, D) were performed. Bar length: 20 μm. Note brush border membrane thinning in *Gcdh*$^{-/-}$ mice treated with HPD (D).

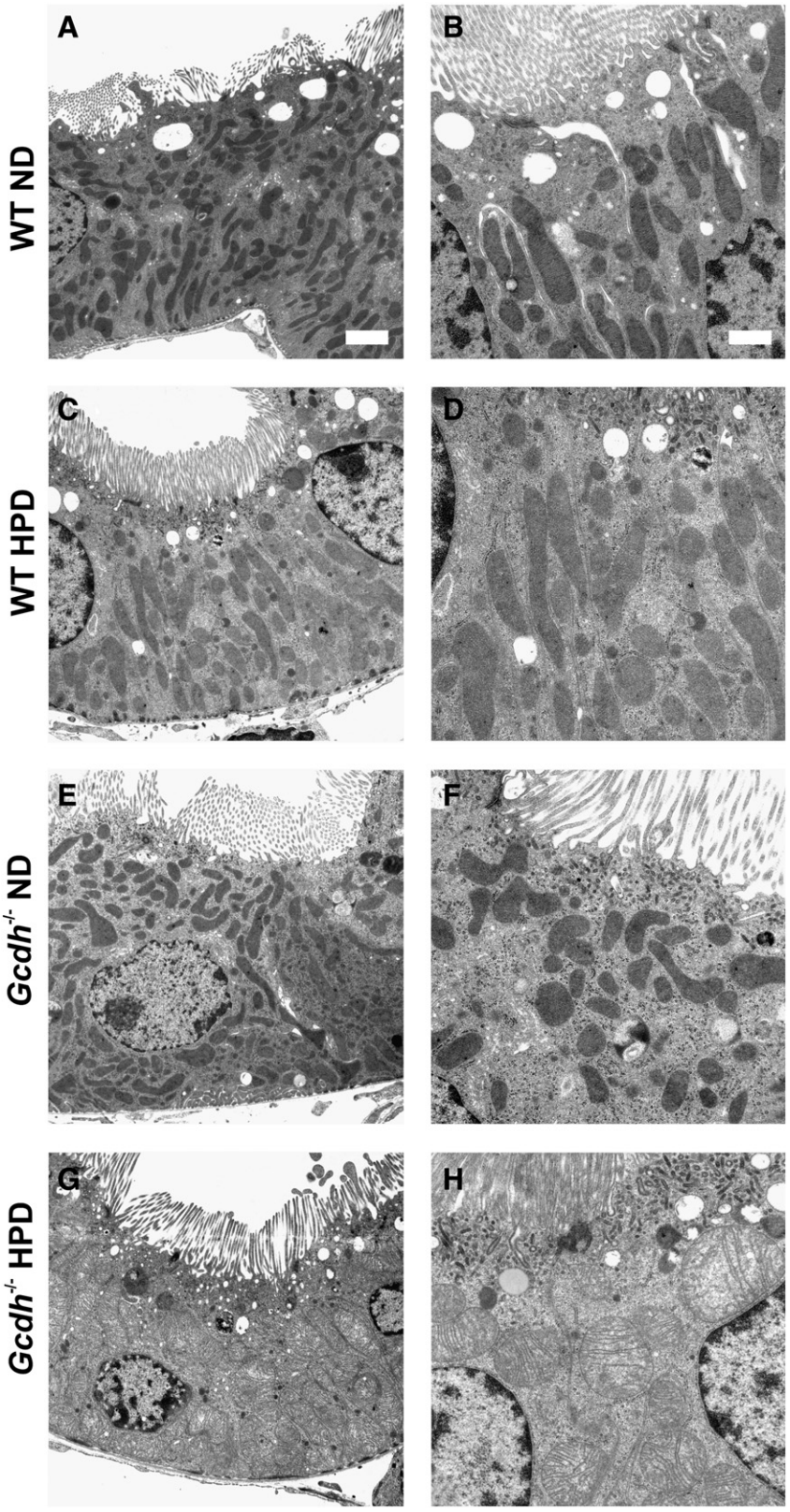

Fig. 6. Electron microscopic evaluation of kidney proximal tubules. Ultrathin kidney sections (60 nm) from wild-type (A–D) and *Gcdh*$^{-/-}$ (E–H) mice kept on ND or four days on HPD were examined by electron microscopy. Magnification: ×7000 (A, C, E, G; bar length 2 μm), ×12,000 (B, D, F, H; bar length 1 μm). Notably, electron micrographs revealed an enlargement as well as a reduced electron density of mitochondria in kidney proximal tubule cells from HPD-treated *Gcdh*$^{-/-}$ mice (G, H) as compared to the other conditions tested.

renal proximal tubule cells, and iii) histomorphological changes in the kidney contributing to functional tubulopathy during induced metabolic crises in *Gcdh*$^{-/-}$ mice.

Previously, we identified NaC3, OAT1 and OAT4 as being capable of transporting GA and 3OHGA in a concerted action from the basolateral to the apical site of renal proximal tubule cells, thus facilitating their

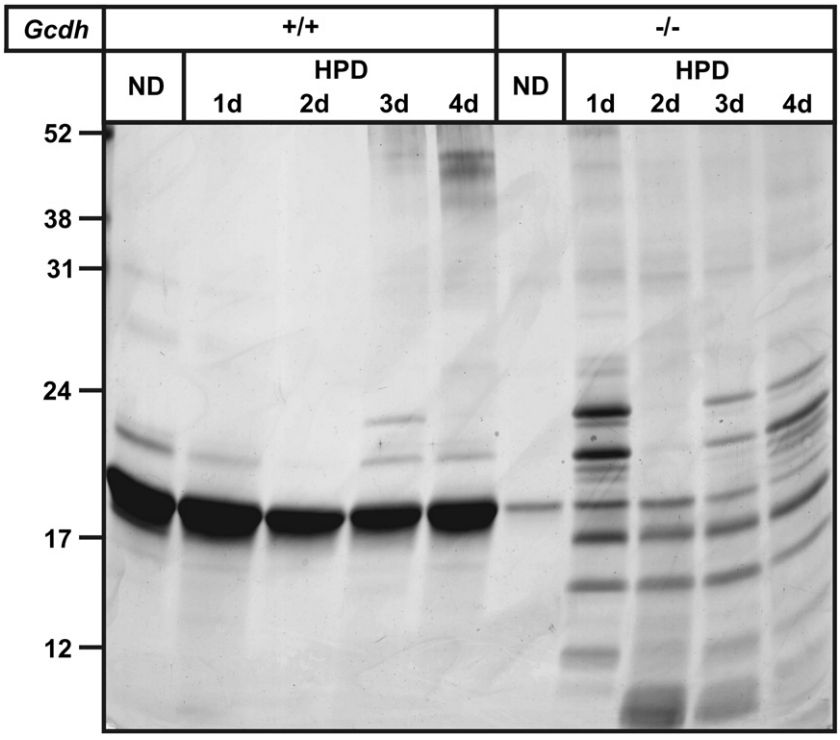

Fig. 7. Protein excretion into urine of HPD-treated mice. 24 h urine was collected from *Gcdh*-deficient (−/−) and wild-type (+/+) mice during ND and HPD administered for four days. Aliquots (1 μg creatinine) were separated by SDS-PAGE and visualized by silver staining. The positions of molecular mass marker proteins (in kDa) are indicated.

urinary excretion [11,12,20]. Here we found that in addition to *NaC3* [11], the *Oat1* mRNA level was significantly increased in kidneys of 42 day-old *Gcdh*$^{-/-}$ mice. OAT1 is capable of transporting GA and 3OHGA with high affinity across membranes [12]. However, NaC3 binds GA and 3OHGA with low affinity [11], and is believed to primarily mediate the uptake of α-ketoglutarate at the basolateral membrane [21], which is required indirectly for the secretion of a variety of organic anions [22]. The increased expression of both NaC3 and OAT1 in kidneys of *Gcdh*$^{-/-}$ mice appears to be an adaptive response to the increased plasma levels of GA and 3OHGA [10]. OAT2, the murine homolog of human OAT4 that is localized at the apical membrane and involved in excretion of organic anions, as well as two unrelated transporters were not altered in their expression (Fig. 8A, B).

Upon high protein diet (HPD) young *Gcdh*$^{-/-}$ mice develop severe catabolic crises within four days of treatment, resembling findings in GA1 patients [9,10]. The crisis is accompanied by a further increase of GA and 3OHGA in body fluids and tissues of *Gcdh*$^{-/-}$ mice, leading to death within 4–5 days [10]. When *Gcdh*$^{-/-}$ mice exposed to HPD were intravenously injected with [^{3}H]-3OHGA, high amounts of radioactivity were found in kidneys [10], suggesting that under conditions of HPD either the uptake of 3OHGA into kidney cells is increased, the excretion rate is decreased, or both occur simultaneously. The mRNA levels,

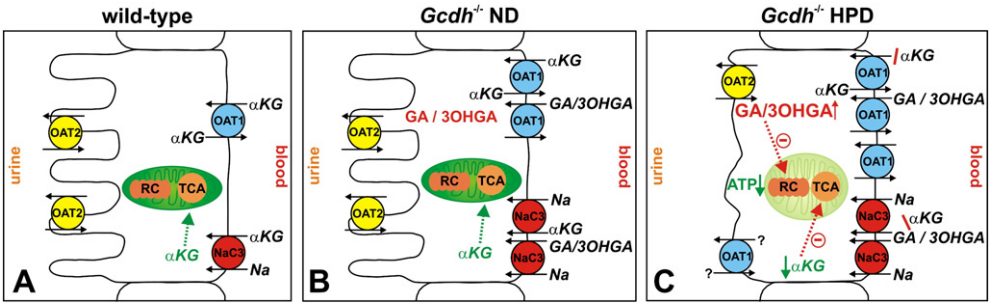

Fig. 8. Model of proximal tubule cell alterations during induced metabolic crises in *Gcdh*$^{-/-}$ mice. (A) In wild-type mice, OAT1 and NaC3 are expressed at the basolateral, OAT2 at the apical membrane. NaC3 mediates the sodium-dependent influx of dicarboxylates such as α-ketoglutarate (αKG) and tricarboxylic acid cycle (TCA) intermediates used as anaplerotic substrates for the TCA cycle [22,31]. (B) *Gcdh*$^{-/-}$ mice under basal conditions on a normal diet (ND) show an upregulation of NaC3 and OAT1, which may represent an adaptive response to increased concentrations of the pathologic metabolites GA and 3OHGA. NaC3 and OAT1 are capable to mediate the basolateral uptake of GA and 3OHGA into proximal tubule cells. OAT2 as the murine ortholog to human OAT4 is a likely candidate for the excretion of GA and 3OHGA into urine at the apical membrane [12]. (C) Under conditions of metabolic crises in *Gcdh*$^{-/-}$ mice induced by a high protein diet (HPD), blood concentrations of GA and 3OHGA show a further increase [10], leading to an elevated basolateral uptake of GA and 3OHGA into proximal tubule cells mediated by increased numbers of NaC3 and OAT1. In addition to increased basolateral uptake, decreased apical OAT2 expression might contribute to the intracellular accumulation of GA/3OHGA metabolites. GA and 3OHGA may contribute to proximal tubule cell injury by at least two mechanisms: 1. GA and 3OHGA may competitively inhibit the uptake of αKG and TCA cycle intermediates *via* OAT1 and NaC3 into the cells, subsequently 2. affecting respiratory chain (RC) activity and mitochondrial production of energy-rich substrates accompanied by mitochondrial swelling. The associated structural and functional changes (decrease in proximal tubule brush border membrane thickness, and low molecular weight proteinuria) may contribute to acute injury of the renal proximal tubule cell in *Gcdh*$^{-/-}$ mice. The role of OAT1 dislocalized to the apical membrane remains unclear.

however, of the basolaterally localized *Oat1* and the apical *Oat2* were observed to be decreased by 50 and 74%, respectively, in kidneys of *Gcdh*$^{-/-}$ mice on HPD. The transcriptional regulation of OAT1, OAT3, and OAT4 in kidneys is coordinated by hepatocyte nuclear factor (HNF) 1α, HNF1β, and HNF4α [23–25]. The signal cascade initiating the transactivation of OATs by HNFs under HPD remains to be studied. The OAT1 protein expression, however, was further augmented in kidneys of *Gcdh*$^{-/-}$ mice in comparison to animals treated with ND, which may explain the elevated uptake of [^{3}H]-3OHGA into kidney cells of HPD-treated *Gcdh*$^{-/-}$ mice [10]. On the other hand, HPD led to a mislocalization of OAT1 to apical membranes of proximal tubule cells, which might impair the turnover resulting in a decreased degradation rate of the OAT1 protein (Fig. 8C). The polarized distribution and function of OATs in proximal tubule cells are mediated by interaction with PDZ (PSD-95/Dlg/ZO-1) domain-containing proteins, such as NHERF-1 and -3 [26]. Thus, NHERF-1 is responsible for apical targeting and trafficking and enhances OAT4-mediated transport activity [27], whereas OAT1 contains a NHERF-3 consensus binding motif (QQL) in its C-terminal cytosolic domain mediating its basolateral localization. In response to changes in intracellular second messenger concentrations and subsequent phosphorylation of NHERFs by protein kinases C and A [28,29], OATs are either inserted into or retrieved from the cell surface. The signaling processes resulting in dislocalization of OAT1 to apical membranes of proximal tubule cells in HPD-treated *Gcdh*$^{-/-}$ mice will be investigated in future studies.

The HPD-induced metabolic crises led to both structural and functional changes in the kidney, including a decrease in proximal tubule brush border membrane thickness, mitochondrial swelling, and a low molecular weight proteinuria in *Gcdh*$^{-/-}$ mice suggesting the presence of an acute tubular injury. The mechanism(s) *via* which accumulating GA and 3OHGA metabolites affect proximal tubule cells remain unclear. It has been suggested that in addition to excitotoxicity and oxidative stress, GA and 3OHGA may impair indirectly the mitochondrial energy metabolism [30] by *e.g.* interference with transport processes essential for the maintenance of cellular functions. Thus, similarly to the inhibition of the dicarboxylate transporter-mediated anaplerotic supply of tricarboxylic acid cycle intermediates from astrocytes to neurons by GA and 3OHGA [7], the metabolites may contribute to mitochondrial energy depletion and cell death in proximal tubule cells. The decreased excretion into the urine of the nutrient and energy-controlled MUP1 in *Gcdh*$^{-/-}$ mice, both under conditions of ND and HPD, further supported the pathomechanistic concept of primary mitochondrial dysfunction in GA1, encompassing proximal tubular cells.

Taken together, the present data provide evidence of dysregulated expression of transporters involved in the translocation of the cytotoxic metabolites GA and 3OHGA in proximal tubule cells during metabolic crises in *Gcdh*$^{-/-}$ mice. The altered expression pattern of these transporters and resulting changes in cytotoxic metabolite levels may contribute to mitochondrial dysfunction and subsequent acute tubular injury in the GA1 mouse model. Future studies will be required to determine whether similar effects on proximal tubule cell function occur in human patients with GA1.

Acknowledgements

This work was supported by Deutsche Forschungsgemeinschaft, grants MU 1778/2-1 and MU 1778/2-2 (to C.M. and J.L.). We thank Chudamani Raithore for excellent technical assistance with electron microscopy.

Disclosure

All authors declare that they have no conflict of interest, and that they have no financial interest in the information contained in the present manuscript.

Appendix A. Supplementary data

Supplementary data to this article can be found online at http://dx.doi.org/10.1016/j.bbadis.2013.04.019.

References

[1] S.I. Goodman, F.E. Frerman, Organic acidemias due to defects in lysine oxidation: 2-ketoadipic acidemia and glutaric acidemia, in: C.R. Scriver, A.L. Beaudet, W.S. Sly, D. Valle, B. Childs, K.W. Kinzler, B. Vogelstein (Eds.), The Metabolic and Molecular Bases of Inherited Disease, McGraw-Hill Inc., New York, USA, 2001, pp. 2195–2204.
[2] S. Kölker, E. Christensen, J.V. Leonard, C.R. Greenberg, A. Boneh, A.B. Burlina, A.P. Burlina, M. Dixon, M. Duran, A. García Cazorla, S.I. Goodman, D.M. Koeller, M. Kyllerman, C. Mühlhausen, E. Müller, J.G. Okun, B. Wilcken, G.F. Hoffmann, P. Burgard, Diagnosis and management of glutaric aciduria type I — revised recommendations, J. Inherit. Metab. Dis. 34 (2011) 677–694.
[3] K. Ullrich, B. Flott-Rahmel, P. Schluff, U. Musshoff, A. Das, T. Lücke, R. Steinfeld, E. Christensen, C. Jakobs, A. Ludolph, A. Neu, R. Röper, Glutaric aciduria type I: pathomechanism of neurodegeneration, J. Inherit. Metab. Dis. 22 (1999) 392–403.
[4] S. Kölker, D.M. Koeller, J.G. Okun, G.F. Hoffmann, Pathomechanisms of neurodegeneration in glutaryl-CoA dehydrogenase deficiency, Ann. Neurol. 55 (2004) 7–12.
[5] C. Mühlhausen, N. Ott, F. Chalajour, D. Tilki, F. Freudenberg, M. Shahhossini, J. Thiem, K. Ullrich, T. Braulke, S. Ergün, Endothelial effects of 3-hydroxyglutaric acid: implications for glutaric aciduria type I, Pediatr. Res. 59 (2006) 196–202.
[6] S.W. Sauer, J.G. Okun, M.A. Schwab, L.S. Crnic, G.F. Hoffmann, S.I. Goodman, D.M. Koeller, S. Kölker, Bioenergetics in glutaryl-CoA dehydrogenase deficiency: a role for glutaryl-coenzyme A, J. Biol. Chem. 280 (2005) 21830–21836.
[7] J. Lamp, B. Keyser, D.M. Koeller, K. Ullrich, T. Braulke, C. Mühlhausen, Glutaric aciduria type 1 metabolites impair the succinate transport from astrocytic to neuronal cells, J. Biol. Chem. 286 (2011) 17777–17784.
[8] D.M. Koeller, M. Woontner, L.S. Crnic, B. Kleinschmidt-DeMasters, J. Stephens, E.L. Hunt, S.I. Goodman, Biochemical, pathologic and behavioral analysis of a mouse model of glutaric acidemia type I, Hum. Mol. Genet. 11 (2002) 347–357.
[9] W.J. Zinnanti, J. Lazovic, E.B. Wolpert, D.A. Antonetti, M.B. Smith, J.R. Connor, M. Woontner, S.I. Goodman, K.C. Cheng, A diet-induced mouse model for glutaric aciduria type I, Brain 129 (2006) 899–910.
[10] B. Keyser, M. Glatzel, F. Stellmer, B. Kortmann, Z. Lukacs, S. Kölker, S.W. Sauer, N. Muschol, W. Herdering, J. Thiem, S.I. Goodman, D.M. Koeller, K. Ullrich, T. Braulke, C. Mühlhausen, Transport and distribution of 3-hydroxyglutaric acid before and during induced encephalopathic crises in a mouse model of glutaric aciduria type 1, Biochim. Biophys. Acta 1782 (2008) 385–390.
[11] F. Stellmer, B. Keyser, B.C. Burckhardt, H. Koepsell, T. Streichert, M. Glatzel, S. Jabs, J. Thiem, W. Herdering, D.M. Koeller, S.I. Goodman, Z. Lukacs, K. Ullrich, G. Burckhardt, T. Braulke, C. Mühlhausen, 3-Hydroxyglutaric acid is transported *via* the sodium-dependent dicarboxylate transporter NaDC3, J. Mol. Med. 85 (2007) 763–770.
[12] Y. Hagos, W. Krick, T. Braulke, C. Mühlhausen, G. Burckhardt, B.C. Burckhardt, Organic anion transporters OAT1 and OAT4 mediate the high affinity transport of glutarate derivatives accumulating in patients with glutaric acidurias, Pflugers Arch. 457 (2008) 223–231.
[13] D. Ballhausen, P. Jafari, L. Bonafé, O. Braissant, Co-expression of GCDH and OAT1 in neurons and proximal tubule cells, J. Inherit. Metab. Dis. 34 (Suppl. 3) (2011) S141.
[14] A.P. Pöge, F. Autschbach, H. Korall, F.K. Trefz, E. Mayatepek, Early clinical manifestation of glutaric aciduria type I and nephrotic syndrome during the first months of life, Acta Paediatr. 86 (1997) 1144–1147.
[15] K.J. Livak, T.D. Schmittgen, Analysis of relative gene expression data using real-time quantitative PCR and the $2^{-\Delta\Delta CT}$ method, Methods 25 (2001) 402–408.
[16] T.N. Meyer, C. Schwesinger, J. Wahlefeld, S. Dehde, D. Kerjaschki, J.U. Becker, R.A. Stahl, F. Thaiss, A new mouse model of immune-mediated podocyte injury, Kidney Int. 72 (2007) 841–852.
[17] H. Blum, H. Beier, H.J. Gross, Improved silver staining of plant proteins, RNA and DNA in polyacrylamide gels, Electrophoresis 8 (1987) 93–99.
[18] M. Ljubojevic, D. Balen, D. Breljak, M. Kusan, N. Anzai, A. Bahn, G. Burckhardt, I. Sabolic, Renal expression of organic anion transporter OAT2 in rats and mice is regulated by sex hormones, Am. J. Physiol. Renal Physiol. 292 (2007) F361–F372.
[19] M. Hosoyamada, K. Ichida, A. Enomoto, T. Hosoya, H. Endou, Function and localization of urate transporter 1 in mouse kidney, J. Am. Soc. Nephrol. 15 (2004) 261–268.
[20] C. Mühlhausen, B.C. Burckhardt, Y. Hagos, G. Burckhardt, B. Keyser, Z. Lukacs, K. Ullrich, T. Braulke, Membrane translocation of glutaric acid and its derivatives, J. Inherit. Metab. Dis. 31 (2008) 188–193.
[21] X. Bai, X. Chen, Z. Feng, K. Hou, P. Zhang, B. Fu, S. Shi, Identification of basolateral membrane targeting signal of human sodium-dependent dicarboxylate transporter 3, J. Cell. Physiol. 206 (2006) 821–830.
[22] B.C. Burckhardt, G. Burckhardt, Transport of organic anions across the basolateral membrane of proximal tubule cells, Rev. Physiol. Biochem. Pharmacol. 146 (2003) 95–158.
[23] L. Jin, R. Kikuchi, T. Saji, H. Kusuhara, Y. Sugiyama, Regulation of tissue-specific expression of renal organic anion transporters by hepatocyte nuclear factor 1 α/β and DNA methylation, J. Pharmacol. Exp. Ther. 340 (2012) 648–655.
[24] K. Ogasawara, T. Terada, J.-i. Asaka, T. Katsura, K.-i. Inui, Hepatocyte nuclear factor-4α regulates the human organic anion transporter 1 gene in the kidney, Am. J. Physiol. Renal Physiol. 292 (2007) F1819–F1826.

[25] T.F. Gallegos, G. Martovetsky, V. Kouznetsova, K.T. Bush, S.K. Nigam, Organic anion and cation SLC22 "drug" transporter (Oat1, Oat3, and Oct1) regulation during development and maturation of the kidney proximal tubule, PLoS One 7 (2012) e40796.
[26] R. Cunningham, R. Biswas, D. Steplock, S. Shenolikar, E. Weinman, Role of NHERF and scaffolding proteins in proximal tubule transport, Urol. Res. 38 (2010) 257–262.
[27] H. Miyazaki, N. Anzai, S. Ekaratanawong, T. Sakata, H.J. Shin, P. Jutabha, T. Hirata, X. He, H. Nonoguchi, K. Tomita, Y. Kanai, H. Endou, Modulation of renal apical organic anion transporter 4 function by two PDZ domain-containing proteins, J. Am. Soc. Nephrol. 16 (2005) 3498–3506.
[28] E.J. Weinman, R.S. Biswas, Q. Peng, L. Shen, C.L. Turner, X. E, D. Steplock, S. Shenolikar, R. Cunningham, Parathyroid hormone inhibits renal phosphate transport by phosphorylation of serine 77 of sodium-hydrogen exchanger regulatory factor-1, J. Clin. Invest. 117 (2007) 3412–3420.
[29] S.A. Barros, C. Srimaroeng, J.L. Perry, R. Walden, N. Dembla-Rajpal, D.H. Sweet, J.B. Pritchard, Activation of protein kinase Cζ increases OAT1 (SLC22A6)- and OAT3 (SLC22A8)-mediated transport, J. Biol. Chem. 284 (2009) 2672–2679.
[30] P. Jafari, O. Braissant, L. Bonafé, D. Ballhausen, The unsolved puzzle of neuropathogenesis in glutaric aciduria type I, Mol. Genet. Metab. 104 (2011) 425–437.
[31] B.C. Burckhardt, J. Lorenz, C. Kobbe, G. Burckhardt, Substrate specificity of the human renal sodium dicarboxylate cotransporter, hNaDC-3, under voltage-clamp conditions, Am. J. Physiol. Renal Physiol. 288 (2005) F792–F799.